Theoretical analysis of a bimode laser

V. Zehnlé*

Laboratoire de Spectroscopie Hertzienne, Unité Associée au CNRS (URA 249), Centre d'Etudes et Recherches sur les Lasers et leurs Applications, Université des Sciences et Technologies de Lille, F-59655 Villeneuve d'Ascq Cedex, France

(Received 26 November 1996; revised manuscript received 29 July 1997)

We study analytically the dynamical behaviors of class *A* and *B* lasers operating on two transverse modes. A generalization of the well-known multimode model of Lamb, taking into account the transverse hole burning effects as well as nonlinear phase couplings, is considered. Taking as a control parameter the difference between the empty cavity eigenfrequency of the modes, the main developments of this article are the following. The existence and stability of stationary patterns related to (i) single-mode stationary states and (ii) locked bimode phase-sensitive solutions are analyzed. (iii) Unlocked periodic behavior and frequency pushing or pulling effects are characterized in a fully analytical description. Our analysis puts in evidence the qualitative differences of stationary as well as periodic behaviors for class *A* and *B* bimodal lasers. Moreover, we show that the laser response is strongly dependent on the symmetry properties, or on the relative spatial parity, of the modes involved: The dynamical properties of opposite or equal parity modes laser are introduced and investigated here. [S1050-2947(98)06401-4]

PACS number(s): 42.55.−f

I. INTRODUCTION

The spatiotemporal dynamics of lasers and the formation of transverse patterns has been a subject of extensive theoretical and experimental [1–5] research for the past ten years. A theoretical approach of these lasers is provided by the Maxwell-Bloch equations (MBE). In order to describe the transverse Gaussian profile of the laser beam, the usual plane-wave approximation is released and the transverse effects are taken into account by a diffraction term in the MBE [6]. In this framework, a lot of theoretical works have been devoted to the study of pattern formation, defects, and spatiotemporal chaos [7–9]. On the other hand, for weakly multimode lasers or low Fresnel number configuration, a simplification of the MBE is provided by the so-called modal approach and was proved efficient for the investigation of spatiotemporal dynamics in lasers [10–13].

The study of mode interaction is a rather old problem in laser physics. Indeed, remembering that each mode is an oscillator characterized by its empty cavity eigenfrequency, these lasers exhibit the general properties of coupled oscillators systems. The laser output intensity oscillate according to the modes beat component corresponding to the frequency differences between the modes that come into play. On the other hand, in the nearly degenerate case, i.e., if the eigenfrequencies of the modes are close enough, locked behavior leading to a stationary intensity output is observed [14]. This phenomenon was termed as cooperative frequency locking by Lugiato *et al.* [15].

Theoretical descriptions of multimode laser oscillators have been developed since the early 1960s. The well-known developments of Lamb [16] for multiple longitudinal modes lasers lead to a set of equations for modal intensities with nonlinearities related to self- and cross-saturation effects. The longitudinal-multimode equations derived by Tang *et al.* [17] for the case of a Fabry-Pérot cavity takes into account the longitudinal holes burned in the inversion by the standing-wave field. As pointed out by Mandel *et al.* [18], this model couples the modal intensities to the population inversion and neglects phase interaction. A recent generalization of the model of Tang *et al.*, which retains phase-sensitive interactions, has been considered in the work of Mandel *et al.* and shows that nonlinear phase coupling leads to important effects notably in semiconductor lasers.

The present work reports on theoretical results for lasers operating on two transverse modes and is motivated by recent experimental observations on the so-called bimode one-dimensional (1D) lasers [19]. These lasers are operating on the transverse Hermite-Gauss TEM_{mn} with $n=0$ modes: As the structure is forced to be purely Gaussian in one direction, the transverse dynamics is in a sense reduced to only one direction, thus justifying the term 1D (the corresponding experimental setup is obtained by putting an intracavity diaphragm of rectangular shape, the smaller size being roughly equal to the laser waist and has been realized on a CO_2 laser [19]). The 1D intensity profile has been recorded and analyzed taking the cavity length L as a control parameter. Apart from the general behaviors of bimode lasers, i.e., locked and oscillatory states, the system is also characterized by the following qualitative properties. It appears that, when stationary, the intensity profile shape changes in a continuous way while changing L. On the other hand, outside the locked region, the intensity behaves periodically in time in a way related not only to beat between the modes but also to the periodic modulation of the modal intensities themselves [5].

In this article we want to characterize analytically these dynamical behaviors of bimodal lasers and perform their critical analysis with respect to laser parameters. With this aim, we consider here the theoretical developments in the framework of a model developed by Stalunias *et al.* [10]. This model describes transverse modes interactions for lasers

*Electronic address: zehnle@lsh.univ-lille1.fr

in a ring cavity configuration and takes account of nonlinear transverse hole-burning effects and of nonlinear phase couplings. The guiding scheme leading to the model of Stalunias *et al.* is reported in Sec. II. In this framework, and in close connection with the experimental findings, a theoretical analysis is performed by taking the difference between the empty cavity eigenfrequencies Ω as a control parameter.

In this article the main developments are the following. We analyze the stationary intensity states corresponding to phase-dependent bimode stationary states and monomode solutions in Sec. III. Section IV deals, in the parameter region of high Ω, with the study of the periodic states. The explicit analytical characterization of beating effects associated with frequency pulling or pushing phenomena and of the oscillatory character of the modal intensities are given. All these behaviors are shown to be critically related to what is termed by Mandel *et al.* as ''phase-sensitive'' effects. Moreover, we show that the laser response depends on the nature, or the relative spatial parity, of the modes that come into play. This is one of the main points of our analytical study and leads to the introduction of what we shall define as ''opposite parity modes'' and ''equal parity modes'' lasers.

II. THEORETICAL DESCRIPTION

We consider a bimode class A or B laser whose spatiotemporal behavior is governed by the mutual interaction of two transverse modes denoted $B_1(x,y)$ and $B_2(x,y)$, where x and y are the Cartesian coordinates in the transverse plane (i.e., perpendicular to the axis z of the cavity). For the sake of simplicity, we suppose here that the functions B_i are real; they correspond, for instance, to the Hermite-Gauss TEM_{mn} modes or to the Laguerre-Gauss modes. The laser field E is

$$E(x,y,z,t)=F(x,y,t)e^{i(k_a z-\omega_a t)}+\text{c.c.}, \tag{2.1}$$

where F is the slowly varying envelope of the field and is, in the mean-field limit, independent of z (ω_a is the atomic frequency and k_a is the related wave vector). The modal expansion considered here is given in detail in [6]. The envelope F is written as

$$F(x,y,t)=g_1(t)B_1(x,y)+g_2(t)B_2(x,y), \tag{2.2}$$

where $g_1(t)$ and $g_2(t)$ are the complex modal amplitudes of modes B_1 and B_2, respectively. The temporal evolution of these amplitudes is governed by

$$\frac{dg_i}{dt}=-\kappa\left[(1+ia_i)g_i-A\int\int B_i(x,y)P(x,y,t)dx\ dy\right],$$

$$i=1,2, \tag{2.3}$$

where κ is the field relaxation rate, A is the pump parameter, and $P(x,y,t)$ is the polarization of the active medium. The parameter

$$a_i=\frac{\omega_i-\omega_a}{\kappa} \tag{2.4}$$

is the detuning of the B_i cavity mode frequency ω_i with respect with to the atomic frequency. Equation (2.3) is coupled to the Bloch equations for the active medium. In the case of class A or B lasers, i.e., when κ and the population inversion decay rate $\gamma_\parallel$ are both small quantities compared to the polarization decay rate $\gamma_\perp$, the adiabatic elimination of P is performed

$$P=FD \tag{2.5}$$

and the population inversion D obeys

$$\frac{dD}{dt}=-\gamma_\parallel(|F|^2D+D-1). \tag{2.6}$$

The population inversion D for class A lasers near threshold can be adiabatically eliminated and written as

$$D(x,y,t)=1-|F|^2=1-\sum_{i,j=1,2} g_i(t)g_j^*(t)B_i(x,y)B_j(x,y). \tag{2.7}$$

According to Stalunias *et al.* [10], Eq. (2.7) can be generalized for class B lasers as:

$$D(x,y,t)=1-\sum_{i\leqslant j=1,2} d_{ij}(t)B_i(x,y)B_j(x,y), \tag{2.8}$$

corresponding to a truncated expansion of D in terms of real time-dependent moments $d_{ij}(t)$. This expansion is valid for small intensity $I=|F|^2$, i.e., near threshold, and accounts for the first-order saturation effects. The modal-like expansion of D leads to a major simplification of the integro-differential equation (2.3). Inserting Eq. (2.8) into Eqs. (2.3) and (2.6) leads to the set of ordinary differential equations (the overdot stands for the derivative with respect to time, where time is in κ^{-1} unit and $\gamma_\parallel$ is in κ unit)

$$\dot{g}_i=-(1+ia_i-A)g_i-A\sum_{m,k\leqslant l} G_{iklm}d_{kl}g_m,$$

$$\dot{d}_{ii}=\gamma_\parallel(d_{ii}-|g_i|^2), \quad i=1,2 \tag{2.9}$$

$$\dot{d}_{12}=\gamma_\parallel(d_{12}-g_1g_2^*-g_2g_1^*),$$

where

$$G_{ijkl}=\int\int dx\ dy\ B_iB_jB_kB_l, \quad i,j,k,l,=1,2 \tag{2.10}$$

are overlap integrals that are related to self-saturation and cross-saturation nonlinear coupling terms. Indeed, if overlap integrals between two modes vanish, cross-saturation terms disappear in Eq. (2.9) and both modes are decoupled. One then obtains the usual set of equations describing a single mode laser. This situation is met, for instance, for a laser operating on a high-order mode together with a low order (i.e., for the TEM_{mn}-TEM_{pq} case with m,n low and p,q high). On the other hand, if the two modes have a high spatial overlap, one recovers the strong-coupling limit where they are in competition for the available inversion.

Let us define the complex modal amplitudes G_i as

$$G_i = A_i e^{i\phi_i} = \sqrt{\frac{A}{A-1}} g_i , \tag{2.11}$$

where A_i and ϕ_i are the real amplitude and phase of mode i. We also rescale the population inversion as

$$D_{ij} = \frac{A}{A-1} d_{ij} \tag{2.12}$$

and define the relative phase between the modes as

$$\phi = \phi_1 - \phi_2 . \tag{2.13}$$

Equations (2.9) become

$$\begin{aligned}
\dot{A}_i &= (A-1)\left[A_i - \sum_{j \leqslant k} G_{ijki} D_{jk} A_i \right. \\
&\left. - \sum_{j \leqslant k} G_{i\bar{i}\bar{j}k} D_{jk} A_{\bar{i}} \cos\phi \right], \quad \bar{i} = 3 - i, \\
\dot{D}_{ii} &= -\gamma_{\parallel}(D_{ii} - A_i^2), \\
\dot{D}_{12} &= -\gamma_{\parallel}(D_{12} - 2A_1 A_2 \cos\phi), \\
\dot{\phi} A_1 A_2 &= \Omega A_1 A_2 + (A-1)(A_1^2 + A_2^2) \sum_{j \leqslant k} G_{12jk} D_{jk} \sin\phi,
\end{aligned} \tag{2.14}$$

where

$$\Omega = a_2 - a_1 \tag{2.15}$$

is the empty cavity frequency difference between the modes. This set of six coupled equations for the modal amplitudes, inversion moments, and phase explicitly takes into account the nonlinear phase couplings. The usual assumptions found in Refs. [16,17] amount to neglecting fast oscillations terms such as $\cos\phi$ or $\sin\phi$ in Eqs. (2.14). One then obtains a set of equations that couples the modal intensities A_i and inversion with no phase interaction. Note that the Lamb model for a bimode laser can be obtained from this model by adiabatically eliminating the inversion variables in Eqs. (2.14) (see Appendix B). One can see that phase couplings, though vanishing in the limit of high Ω, are non-negligible for intermediate Ω values (see Sec. IV) and are indeed important for the study of the stationary states in the locked region ($\dot{\phi} = 0$).

One of the main results of this paper is related to the nature of the modes that come into play. A simplification of Eqs. (2.9) or (2.14) occurs when the two modes involved in the equations have opposite spatial parity (with respect to space inversion). To make things clearer, let us consider, for instance, the case of the 1D transverse lasers. The modes B_i ($i = 1,2$) are the Gauss-Hermite $\mathrm{TEM}_{m_i 0} \equiv \mathrm{TEM}_{m_i, n=0}$ modes [20]

$$B_i(x,y) = \sqrt{\frac{1}{\pi m_i ! 2^{m_i - 1}}} H_{m_i}(\sqrt{2}x) e^{-(x^2+y^2)}, \tag{2.16}$$

corresponding to a Gaussian shape in the y direction, the so-called 1D structure associated with the Hermite polynomial of order m_i being related to the x direction. The modes B_i are odd or even in x if the corresponding index m_i is odd or even. Consequently, overlap integrals such as G_{1112} (G_{2221}) with m_1 odd (even) and m_2 even (odd) are zero. More generally, let us also note that the same symmetry effect is found in a 2D laser such as the TEM_{mn}-$\mathrm{TEM}_{m'n'}$ bimode laser with $m+m'$ or $n+n'$ odd. This type of laser has its behavior qualitatively modified as a result of vanishing cross couplings [corresponding to the G_{iiij}, $j \neq i$, terms in Eqs. (2.14)]. The comparison between what we call here opposite parity modes (OPMs) and equal parity modes (EPMs) lasers is developed in the following sections.

III. THEORETICAL ANALYSIS OF THE STATIONARY STATES

The analysis of bimode stationary behavior is hard to handle in the general case. In the first part of this section we consider a simplification of model (2.14) for a particular ''symmetrical'' OPM case. This case, though simple, can be treated analytically and puts in evidence the generic properties of the general bimode laser. This general case is considered next. The stationary OPM and EPM bimode lasers are studied in the limit where the empty cavity mode frequencies a_i are quasidegenerate, i.e., when $\Omega \to 0$. An alternative stationary state is provided by the single-mode solution (A_1 or $A_2 = 0$) and is studied subsequently.

A. Stationary bimode solution: The symmetrical OPM case

The analysis of stationary solutions is performed in the symmetrical OPM case, i.e., for a laser involving TEM_{mn}-TEM_{nm} ($n+m$ odd) modes, for instance, for the TEM_{01}-TEM_{10} laser. The symmetry property reads $G_{11} = G_{22}$ (G_{ij} stands for G_{iijj}) and parity properties leads to $G_{1112} = G_{2221} = 0$. The stationary variables are found from Eqs. (2.14):

$$\begin{aligned}
G_{12} I_s (G + 1 + 2\cos^2\phi_s) &= 1, \\
G_{12} I_s \sin(2\phi_s) &= -\frac{\Omega}{2(A-1)},
\end{aligned} \tag{3.1}$$

where ϕ_s is the stationary phase and $I_s = A_{1s}^2 = A_{2s}^2$ is the stationary modal intensity equal, for symmetry reason, for both modes and $G = G_{11}/G_{12}$ ($G \geqslant 1$ [21]). A closed equation for ϕ_s can obtained as

$$\cos(2\phi_s - \Phi) = -(2+G)\cos\Phi, \tag{3.2}$$

where

$$\cos\Phi = \frac{\Omega}{\Omega^2 + 4(A-1)^2} \tag{3.3}$$

and $0 \leqslant \Phi \leqslant \pi$. The existence of stationary solutions is found from Eq. (3.3) as long as

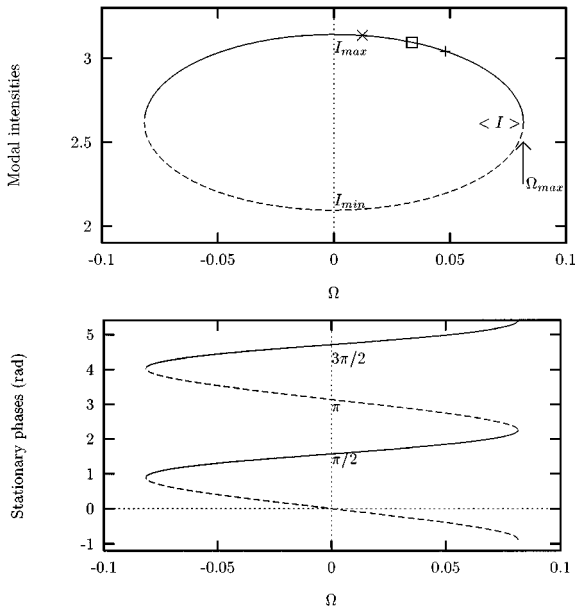

FIG. 1. Stationary intensities and phase for the symmetrical OPM TEM_{01}-TEM_{10} laser vs Ω ($G_{11}=G_{22}=3/4\pi$, $G_{12}=1/4\pi$, and $A=1.2$). Full (dotted) lines are the stable (unstable) branches for class A lasers. $\times$, $\square$, and $+$ correspond to Hopf bifurcation points for $\gamma_\parallel=10^{-3}$, 0.01, and 0.02, respectively.

$$|\Omega| \leqslant \Omega_{max} = \frac{2(A-1)}{\sqrt{(2+G)^2-1}}. \tag{3.4}$$

The phase ϕ_s can be explicited as

$$\phi_s = \frac{\Phi}{2} \pm \frac{1}{2}\arccos[(2+G)\cos\Phi] \pm \frac{\pi}{2}, \tag{3.5}$$

corresponding to four branches of solution in the interval $[0,2\pi]$. The stationary phase and intensity are shown in Fig. 1. Note that both phase branches ($\phi_s, \phi_s+\pi$) correspond to the same intensity branch. In the degenerate case ($\Omega=0$), one gets

$$\begin{aligned} &\phi_s = 0,\pi, \quad I_s = I_{min} = G_{12}^{-1}(G+3)^{-1}, \\ &\phi_s = \pm\pi/2, \quad I_s = I_{max} = G_{12}^{-1}(G+1)^{-1}. \end{aligned} \tag{3.6}$$

For $\Omega=\Omega_{max}$, one finds

$$\phi_s = \frac{1}{2}\arccos\left(\frac{1}{2+G}\right) + \frac{\pi}{2}(\mathrm{mod}\,\pi), \quad I_s = \langle I\rangle = \frac{I_{max}+I_{min}}{2}. \tag{3.7}$$

We have developed the stability analysis for class A lasers (see Appendix A). The upper intensity branch ($\langle I\rangle \leqslant I_s \leqslant I_{max}$) is a branch of stable nodes, while the lower ($I_{min} \leqslant I_s \leqslant \langle I\rangle$) is a branch of hyperbolic points, both branches merging into a saddle node bifurcation point at $\pm\Omega_{max}$.

The analysis for class B lasers has been performed in the limit $\gamma_\parallel/(A-1)\to 0$ (see Appendix A). The lower-intensity branch remains unstable. The upper branch is stable when

$$I_s \geqslant I_{Hopf} = I_{max}\left[1 - \frac{\gamma_\parallel}{2(A-1)}\frac{G-1}{G+1}\right] \tag{3.8}$$

or

$$|\Omega| \leqslant \Omega_{Hopf} = 2\sqrt{\gamma_\parallel(A-1)}\frac{\sqrt{G-1}}{G+1} \tag{3.9}$$

and destabilizes in a Hopf bifurcation when $\Omega=\Omega_{Hopf}$ (numerical continuation of the periodic orbit at Ω_{Hopf} shows that the Hopf bifurcation is subcritical [22]).

We have explicitly shown that the locking threshold is much smaller in class B than in class A lasers: For class A lasers the conditions of existence and stability are simultaneously fulfilled. Class B lasers, on the other hand, exhibit a bimode stable steady state in a small interval around $\Omega=0$ that shrinks to zero with $[\gamma_\parallel(A-1)]^{1/2}$. Let us note that the unlocking threshold Ω_{Hopf} is on the order of the relaxation frequencies associated with class B lasers. The existence of such relaxation eigenfrequencies (and the related resonances) is reponsible for a mechanism of destabilization that makes the stability properties of locked solutions for class B lasers qualitatively different from those for class A lasers.

B. Stationary bimode solution: The general case

The bimode stationary solutions in the degenerate (i.e., $\Omega=0$) OPM case, denoted ϕ_s, A_{1s}, and A_{2s} ($A_{1s}, A_{2s} \neq 0$), read, from Eqs. (2.14),

$$\begin{aligned} &\sin(2\phi_s) = 0, \\ &G_{11}A_{1s}^2 + G_{12}A_{2s}^2(1+2\cos^2\phi_s) = 1, \\ &G_{22}A_{2s}^2 + G_{12}A_{1s}^2(1+2\cos^2\phi_s) = 1 \end{aligned} \tag{3.10}$$

($G_{ij} \equiv G_{iijj}$). The stationary phases ϕ_s are $\phi_s = 0, \pi, \pm\pi/2$. The linear stability analysis of these stationary solutions is reported in Appendix C. It is shown that $\phi_s = 0, \pi$ are unstable solutions, whereas $\phi_s = \pm\pi/2$ are simultaneously stable. For both solutions, the modal intensities $I_i = A_{is}^2$ are given by

$$I_1 = \frac{G_{22}-G_{12}}{G_{22}G_{11}-G_{12}^2}, \quad I_2 = \frac{G_{11}-G_{12}}{G_{22}G_{11}-G_{12}^2}. \tag{3.11}$$

These stationary values are functions of the overlap integrals only. The analogy with the Lamb analysis of a bimode laser is clear from Eqs. (3.11) [assuming $\phi_s = \pm\pi/2$ amounts to neglecting phase couplings in Eqs. (2.14)].

In the following we label 2 the higher-order mode, i.e., the mode with the wider spatial extension or, equivalently, the lower G_{22} value, in contrast to mode 1 which is assumed to have a higher-G_{11} value. I_1 and I_2 are positive quantities [23]. Equations (3.11) together with the assumption $G_{11} \geqslant G_{22}$ show that the higher-mode intensity is always dominant i.e., $I_2 \geqslant I_1$. Let us note here the analogy with the free-energy approach: Qualitatively speaking, the wider mode burns more efficiently the spatially distributed inversion, which leads to a minimization of a particular action integral of the laser [4,24]. Of course, remember the assumptions of

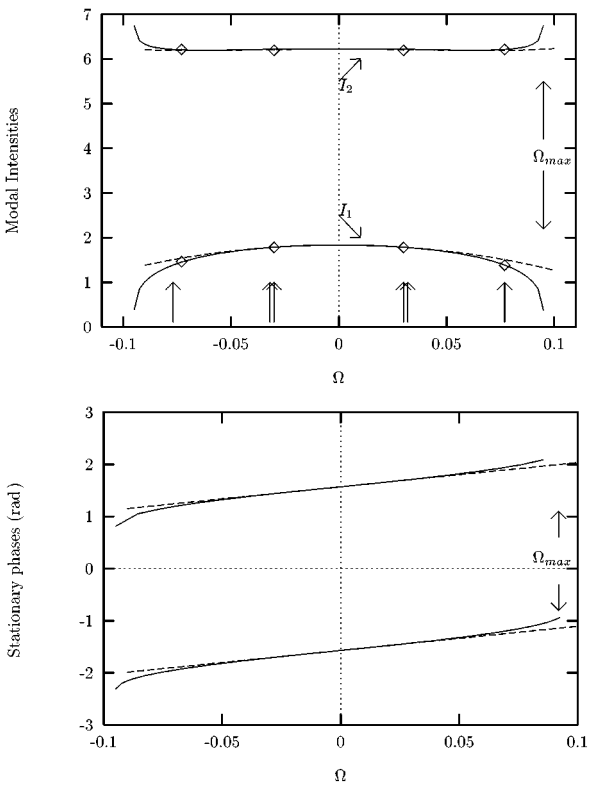

FIG. 2. Stationary modal intensities and phase for the OPM TEM_{00}-TEM_{70} laser vs Ω obtained numerically from Eqs. (2.14). The dotted lines correspond to the theoretical results reported in text. $G_{11}=1/\pi$, $G_{22}=0.443/\pi$, and $G_{12}=0.21/\pi$, where indices 1 and 2 are related to modes TEM_{00} and TEM_{70}, respectively, and $A=1.2$. The existence and stability are found when $\Omega \leqslant \Omega_{max}=0.095$ for class A lasers and the Hopf bifurcation ($\diamond$) related to class B lasers is shown by the arrow (double arrow) for $\gamma_{\parallel}=0.1$ ($\gamma_{\parallel}=0.01$).

the model, i.e., no gain or loss effects favoring one of the mode. Note finally that in the limit of small coupling, i.e., when $G_{12}\rightarrow 0$, one finds the monomode limit $I_i=1/G_{ii}$: The spatial overlap is weak and the modes do not compete for the population inversion.

When $\Omega \neq 0$, the stationary values cannot be explicited exactly. The first-order correction to the phase is given by

$$\phi_s=\pm\frac{\pi}{2}+\delta\phi_s,$$
$$\delta\phi_s=\frac{\Omega}{2(A-1)G_{12}(I_1+I_2)}. \tag{3.12}$$

The correction to I_1 and I_2 is $O(\delta\phi_s^2)$ or, equivalently, $O(\Omega^2)$. The modal intensities are phase dependent [see Eqs. (3.10)] and are given by expressions (3.11) with $G_{12}\rightarrow G'_{12}=G_{12}(1+2\delta\phi_s^2)$.

Somewhat arbitrarily, we have chosen to illustrate our results for a laser, with medium coupling integrals, operating on the TEM_{00} and TEM_{70} modes. Figure 2 corresponds to the analytical values of intensities and phases, respectively. The numerical simulation of Eqs. (2.14) has been performed and is reported in both figures. The theoretical and numerical

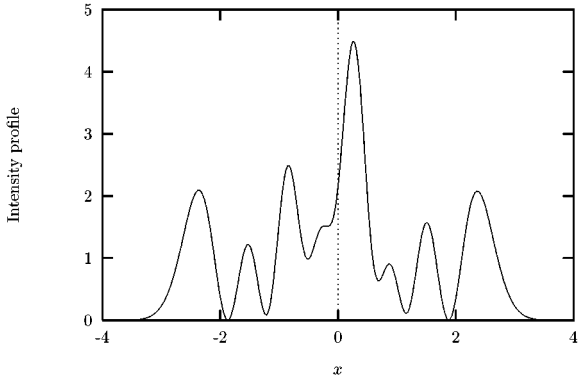

FIG. 3. Stationary intensity profile for the TEM_{00}-TEM_{70} class B laser. Same parameters as in Fig. 2, but $\Omega=0.085$ and $\gamma_{\parallel}=0.1$. The stationary phase is $\phi_s=-0.4\pi$ and the intensities are $I_1=1.7$ and $I_2=6.2$

results are in very good agreement. Note that both branches of stationary phases (branches ϕ_s and $\phi_s+\pi$) correspond to the same modal intensities. The stability analysis of these branches cannot be performed analytically for $\Omega\neq 0$. Numerically, as for the symmetrical case, it is found that the existence and stability of steady states are simultaneously met for class A lasers for $\Omega\leqslant\Omega_{max}$ and that a Hopf bifurcation occurs for class B lasers in the vicinity of $\Omega=0$.

The general expression of the intensity profile $I(x,y)=|F(x,y)|^2$ reads, from Eqs. (2.2) and (2.11),

$$I(x,y)=\frac{A-1}{A}[I_1B_1^2(x,y)+I_2B_2^2(x,y) +2\sqrt{I_1I_2}B_1(x,y)B_2(x,y)\cos\phi]. \tag{3.13}$$

When $\Omega=0$ both stationary values $\phi_s=\pm\pi/2$ lead to the same intensity pattern. In the nondegenerate case, one finds a bistability between two different phase-dependent patterns. Indeed, inserting Eq. (3.12) into Eq. (3.13), one has

$$I(x,y)=\frac{A-1}{A}[I_1^2B_1^2(x,y)+I_2^2B_2^2(x,y) \pm 2\sqrt{I_1I_2}B_1(x,y)B_2(x,y)\sin\delta\phi_s]. \tag{3.14}$$

For 1D lasers, the patterns are not symmetric in the x direction [because of the odd $B_1(x,y)B_2(x,y)$ term]. Figure 3 is the stationary profile for the TEM_{00}-TEM_{70} case, which has been found numerically at $\Omega=0.085$. Due to the symmetry of the model, bistability is found with the reversed (i.e., $x\rightarrow -x$) pattern. It is interesting to note that the intensity profile changes in a continuous way with parameter Ω. This behavior is in qualitative agreement with the experiments reported in [19].

The EPM case is harder to handle analytically and we give just a few results here. From Eqs. (2.14), one straightforwardly finds the following expression for the stationary phases:

$$[G_{1112}A_{1s}^2+G_{2221}A_{2s}^2+2A_1A_2G_{12}\cos\phi_s]\sin\phi_s=0. \tag{3.15}$$

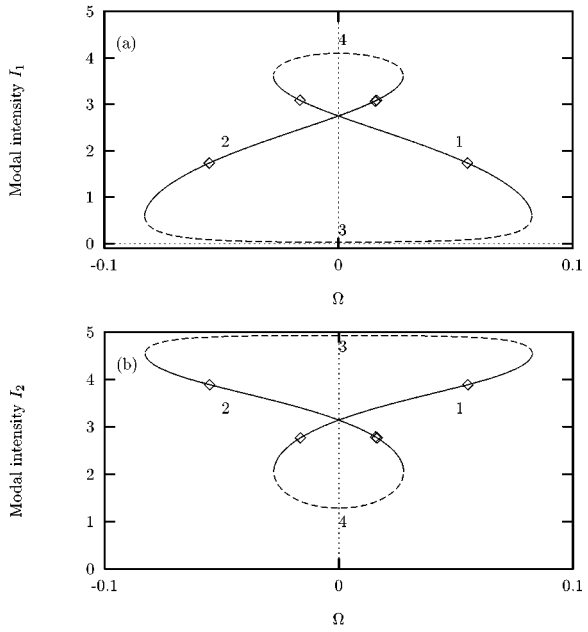

FIG. 4. Stationary modal intensities for the EPM TEM_{00}-TEM_{02} laser vs Ω obtained numerically from Eqs. (2.14): (a) TEM_{00} intensity and (b) TEM_{02} intensity. Full lines (branches labeled 1 and 2) and dotted lines (branches 3 and 4) are related to stable and unstable solutions for the class *A* laser. ◇ are the Hopf bifurcation points for the class *B* laser with $\gamma_\parallel=0.01$. $G_{11}=1/\pi$, $G_{22}=41/64\pi$, $G_{12}=3/8\pi$, $G_{1112}=-\sqrt{2}/4\pi$, and $G_{2221}=\sqrt{2}/32\pi$, where indices 1 and 2 are related to modes TEM_{00} and TEM_{02}, respectively ($A=1.2$).

There are no explicit values of the modal intensities corresponding the branches $\phi_s=0,\pi$. The other solutions, corresponding to the EPM counterpart of Eqs. (3.11), read

$$I_1=\frac{G'_{22}-G'_{12}}{G'_{22}G'_{11}-(G'_{12})^2},\quad I_2=\frac{G'_{22}-G'_{12}}{G'_{22}G'_{11}-(G'_{12})^2},\tag{3.16}$$

$$\cos\phi_s=-\frac{G_{1112}I_1+G_{1222}I_2}{2\sqrt{I_1I_2}G_{12}},$$

where $G'_{11}=G_{11}-G^2_{1112}/G_{12}$, $G'_{12}=G_{12}-G_{1112}G_{1222}/G_{12}$, and $G'_{22}=G_{22}-G^2_{1222}/G_{12}$.

The stability analysis of these solutions is difficult to handle analytically and has not been performed. We just give numerical results in Figs. 4 and 5 for the TEM_{00}-TEM_{20} laser. The main difference is the loss of symmetry $\phi_s\leftrightarrow\phi_s+n\pi$ compared to the OPM case. This leads, for instance, to intensity bistability, as can be seen from Fig. 4. However, here again, the existence and stability for class *A* lasers and the Hopf bifurcation occurrence for small Ω values in class *B* lasers are found.

C. Monomode solution

We now turn our attention to the study of the single-mode stationary intensity. In this framework, it is worth returning back to the set of equations (2.9) with Eqs. (2.11) and (2.12). Let us assume that mode 2 is oscillating and there is a vanishing amplitude for mode 1, i.e., $G_1=0$, $G_2\neq0$, and $|G_2|$ stationary. We find the results

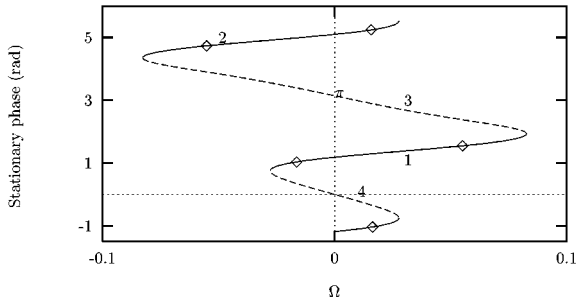

FIG. 5. Stationary phases for the EPM TEM_{00}-TEM_{02} laser vs Ω. Same parameters as in Fig. 4. At $\Omega=0$, $\phi_s=0,\pi$ and $\phi_s\approx\pm3\pi/8$ (mod 2π).

$$G_{1222}|G_2|^2=0,\tag{3.17}$$

$$G_{22}|G_2|^2=1.\tag{3.18}$$

It is interesting to note that these equations are meaningless if $G_{1222}\neq0$ and the EPM laser cannot have a monomode response (unless near threshold, where the model is valid). In the OPM case, one has $G_{1222}\equiv0$ and the stationary state is characterized by

$$|G_2|^2=\frac{1}{G_{22}},\tag{3.19}$$

$$D_{ij}=|G_2|^2\delta_{i,2}\delta_{j,2}.\tag{3.20}$$

The stability analysis of this solution is reported in Appendix D and has been developed for arbitrary Ω. The monomode state remains stable above threshold ($A\geqslant1$) and as long as the following conditions are simultaneously fulfilled:

$$g\leqslant\frac{1}{2},$$

$$(2g-3g^2)\leqslant\left[\frac{\Omega}{(A-1)}\right]^2\leqslant\gamma^2\left(\frac{1}{g}-2\right)+\gamma(3g-1)-g^2,\tag{3.21}$$

where the parameter $\gamma=\gamma_\parallel/(A-1)$. The parameter g ($0\leqslant g\leqslant1$), defined as

$$g=1-\frac{G_{12}}{G_{22}},\tag{3.22}$$

is related to the strength of the interaction between the modes.

In the weak-coupling limit, i.e., when $G_{12}\ll G_{22}$ or $g\to1$, the laser cannot display a stable monomode behavior. The laser with TEM_{01} and TEM_{10} modes with the parameter $g=2/3$ is an example of such a case. Indeed, in this limit the modes do not share the same inversion and oscillate simultaneously above threshold.

Note that class *B* lasers are *a priori* unable to sustain a monomode behavior [see Eq. (3.21) with $\gamma\to0$]. This result might be surprising since monomode class *B* lasers are very

common. However, remember that gain and loss are assumed to be equal for both modes. One could release this symmetry and introduce, for instance, mode-dependent losses κ_i and in this way favor one of the modes. This would obviously lead to stable monomode solutions (in the same way, an intracavity diaphragm can force the laser to operate on the TEM_{00} mode only).

For a class A laser, on the other hand, taking the limit $\gamma \gg 1$, one finds that the monomode solution is stable provided $2g-3g^2 \leqslant \Omega^2/(A-1)^2 \leqslant \gamma^2(1/g-2)$, i.e., for almost all parameter values, provided $g \leqslant 1/2$: For strong coupling or for high spatial overlap one of the modes is built with all the available inversion at the expense of the other. Let us remark that this limit is found for high-order ''neighbor'' modes, for instance, the 1D $TEM_{n,0}$-$TEM_{n+1,0}$ case with $n \gg 1$.

As a final comment let us point out that when $\Omega=0$, it is not possible to find a parameter region in the plane $(g,\gamma_\parallel)$ fulfilling simultaneously the conditions (3.21). The monomode is always unstable in this limit and the laser has the bimode behavior characterized in Sec. III B.

Consider, for instance, the 1D TEM_{00}-TEM_{10} mode ($G_{11}=1/\pi$, $G_{22}=3/4\pi$, $G_{12}=1/2\pi$, and, for instance, $A=1.2$ and $\gamma_\parallel=1$). The TEM_{00} mode ($g=1/2$) is stable for $0.01 \leqslant \Omega^2 \leqslant 0.09$ and the TEM_{10} mode ($g=1/3$) is stable in a wider interval, i.e., for $1.33\times 10^{-2} \leqslant \Omega^2 \leqslant 0.995$.

D. Quasimonomode solution: The EPM case

In the EPM case, it is possible to find solutions with a small amplitude for one mode, the other one having a finite-amplitude value. We mention here briefly the existence of these stationary ''monomodelike'' solutions in the high-Ω limit. Let us consider Eqs. (2.14) and introduce the parameter $\epsilon=(A-1)/\Omega$, $\epsilon \ll 1$. One looks for a solution with small amplitude, say, $A_{1s}=O(\epsilon)$ and $A_{2s}=O(1)$ for mode 2. To leading order this stationary amplitude reads

$$A_{1s}=\frac{|G_{2221}|}{G_{22}^{3/2}}\epsilon+O(\epsilon^2),$$
$$A_{2s}=\frac{1}{G_{22}^{1/2}}+O(\epsilon) \tag{3.23}$$

and the stationary phase is given by $\phi_s=\pm\pi/2$ (where the sign $\pm$ depends on the sign of parameter G_{1112}/G_{2221}). These solutions, corresponding to the EPM monomodelike counterpart of the OPM monomode solutions, were found numerically to be stable for class A lasers (for the TEM_{00}-TEM_{02} case, for instance).

E. Summary

In this section we proved the existence and stability of stationary states of both single mode and bimode types and showed their deep dependence on the parameter Ω. Bimode solutions exist and are always stable in the degenerate case $\Omega=0$. The analysis of the so-called symmetrical OPM class A laser showed the existence and stability of steady states for $\Omega \leqslant \Omega_{max}$ together with a saddle-node bifurcation at Ω_{max}. Destabilization of this steady-state branch or unlocking threshold, via a Hopf bifurcation at $\Omega_{Hopf} \sim \gamma_\parallel^{1/2}$, has been evidenced for class B lasers. These results are generic features of bimode lasers that are also met in the general OPM or EPM case: The unlocking threshold is much smaller in class B than in class A lasers.

We also note that the intensity pattern varies in a continuous way with the parameter Ω. This behavior is clearly related to intermode phase effects and shows the importance of phase-sensitive interactions.

On the other hand, single-mode behavior is found for the OPM lasers. Stability is discussed explicitly with respect to the laser parameters $\gamma_\parallel$, Ω, and coupling strength g: It is shown that single-mode oscillations are behavior for strongly coupled class A lasers in a wide Ω interval. However, for $\Omega=0$, this single-mode state is always unstable and the laser behavior is bimodal. We also noted the existence of EPM ''quasimonomode'' steady states for high Ω.

IV. PERIODIC SOLUTIONS

In the opposite limit of high-Ω values, the modes are well separated in frequency and have a natural tendency to unlock. Moreover, both modes tend to behave as free oscillators (in phase) of pulsations a_1 and a_2, respectively, but still interact since they share the same population inversion. The laser output intensity exhibits a mode beat component corresponding to the frequency difference Ω. As pointed out in Sec. II, the high-Ω periodic state can be obtained to dominant order by neglecting the fast oscillating term in $\cos\phi$ and $\sin\phi$ (where, in this limit, $\phi=\Omega t$) in Eqs. (2.14). In the following, we consider the first-order corrections to this asymptotic behavior and display the analytical description of the following points: (i) the intensity oscillations are related not only to beating but also to the oscillatory character of the modal amplitudes themselves and (ii) the beat frequency is pushed or pulled depending on the laser parameters. These effects are analyzed for the OPM and EPM cases. Due to their different time scales, the cases of class B and A lasers will be considered successively.

A. Class *B* lasers

Let us consider first the class B laser. We assume here that both $A-1$ and $\gamma_\parallel$ are small quantities with respect to Ω and define

$$\frac{A-1}{\Omega}=\epsilon, \tag{4.1}$$

$$\frac{\gamma_\parallel}{A-1}=\gamma, \tag{4.2}$$

where ϵ is a small parameter and γ is assumed to be $O(1)$. Note that the limit $\epsilon \to 0$ in Eq. (4.1) is valid when Ω is $O(1)$ since $A-1$ is assumed to be small in the near-threshold derivation of the model (see Sec. II). In the following, what we call high Ω means high with respect to the parameter $A-1$. In physical units and according to Eqs. (2.4) and (2.15), this condition is fulfilled for lasers with $O(\kappa)$ intermode frequency detuning.

Dividing the set of equations (2.14) by Ω one has

$$\dot{A}_i=\epsilon\left[A_i-\sum_{j\leqslant k}G_{iijk}D_{jk}A_i-\sum_{j\leqslant k}G_{i\,\bar{i}\,jk}D_{jk}A_{\bar{i}}\cos\phi\right],$$

$$\bar{i}=3-i,$$

$$\dot{D}_{ii}=-\gamma\epsilon(D_{ii}-A_i^2),$$

$$\dot{D}_{12}=-\gamma\epsilon(D_{12}-2A_1A_2\cos\phi), \tag{4.3}$$

$$\dot{\phi}=1+\epsilon\frac{(A_1^2+A_2^2)}{A_1A_2}\sum_{j\leqslant k}G_{12jk}D_{jk}\sin\phi,$$

where the overdots stand for derivatives with respect to time $\tau=\kappa\Omega t$. This form is suitable for a perturbative analysis, to which we now turn our attention.

When $\epsilon\ll 1$, the phase behaves as $\phi(t)=t$ and the modal amplitudes A_i and moments D_{ij} are independent of time, as can be seen from Eqs. (4.3). The intensity $I(x,y,t)$ behaves periodically in time with a pulsation $\omega=1$ (in $\kappa\Omega$ units) corresponding to the empty cavity beat frequency between the modes.

In order to take into account the interaction between the modes and look for the first-order corrections to this ''free'' behavior, we emphasize that the phase is given by $\phi(t)=\omega(\epsilon)t$, where the pulsation is expanded as

$$\omega(\epsilon)=1+a\epsilon+b\epsilon^2+O(\epsilon^3), \tag{4.4}$$

where a and b are unknown coefficients. We look for solutions depending on time T, where

$$T=\omega(\epsilon)t=(1+a\epsilon+b\epsilon^2+\cdots)t. \tag{4.5}$$

Expanding the variables in Eqs. (2.14) in power series of ϵ,

$$f(T)=f^{(0)}(T)+\epsilon f^{(1)}(T)+\epsilon^2 f^{(2)}(T)+\cdots,\quad f=A_i,D_{ij},\phi, \tag{4.6}$$

one obtains to dominant order

$$D_{ij}^{(0)}(T)=D_{ij}^{(0)},\quad A_i^{(0)}(T)=A_i^{(0)}, \tag{4.7}$$

and

$$\phi^{(0)}(T)=T, \tag{4.8}$$

where we have assumed, without loss of generality, that $\phi(T=0)=0$. The higher-order expansion is given in detail in Appendix E.

For the EPM case, the solutions of Eqs. (4.3) are given to order ϵ by

$$A_i(T)=A_i^{(0)}-\epsilon\beta A_{\bar{i}}^{(0)}\sin T,$$

$$D_{ii}(T)=I_i^{(0)}+O(\epsilon^2),$$

$$D_{12}(T)=2\epsilon\gamma A_1^{(0)}A_2^{(0)}\sin T, \tag{4.9}$$

$$\phi(T)=T-\epsilon\beta\frac{I_1^{(0)}+I_2^{(0)}}{\sqrt{I_1^{(0)}I_2^{(0)}}}(\cos T-1),$$

where $\beta=\Sigma_j G_{12jj}I_j^{(0)}$ and the $O(\epsilon^0)$ intensities are given by

$$I_1^{(0)}=[A_1^{(0)}]^2=\frac{G_{22}-G_{12}}{G_{22}G_{11}-G_{12}^2},$$

$$I_2^{(0)}=[A_2^{(0)}]^2=\frac{G_{11}-G_{12}}{G_{22}G_{11}-G_{12}^2}. \tag{4.10}$$

For the OPM, $\beta=0$ and the expansion must be developed to higher order. To order ϵ^2 one gets the results

$$A_i(T)=[A_i^{(0)}+\epsilon^2A_i^{(2)}]+\frac{1}{2}\epsilon^2\gamma G_{12}I_{\bar{i}}^{(0)}A_i^{(0)}\cos 2T,$$

$$D_{ii}(T)=I_i^{(0)}+\epsilon^2I_i^{(2)},$$

$$D_{12}(T)=2\epsilon\gamma A_1^{(0)}A_2^{(0)}\sin T+2\epsilon^2\gamma^2A_1^{(0)}A_2^{(0)}\cos T, \tag{4.11}$$

$$\phi(T)=T-\frac{1}{2}\epsilon^2\gamma[I_1^0+I_2^0]\sin(2T).$$

The time-independent amplitudes $A_i^{(0)}$ and intensities $I_i^{(0)}$ are defined by Eqs. (4.10) and the related $O(\epsilon^2)$ corrections are reported in Eqs. (E9) of Appendix E.

As can be seen from these results, the dynamical behavior is extremely sensitive to the relative parity of the two modes involved. Indeed, the mean values of solutions (4.9) and (4.11) are almost the same, but the time dependence is completely different in both cases. Considering the intensities, for instance, one has for the EPM and OPM cases, respectively,

$$I_i(T)=I_i^{(0)}-2\epsilon\beta A_1A_2\sin T+O(\epsilon^2) \tag{4.12}$$

and

$$I_i(T)=I_i^{(0)}+\epsilon^2[2A_i^{(0)}A_i^{(2)}+\gamma I_1^{(0)}I_2^{(0)}\cos 2T]+O(\epsilon^3). \tag{4.13}$$

The modulation is stronger (of order ϵ or Ω^{-1}) in the EPM than in the OPM case (of order ϵ^2 or Ω^{-2}). Moreover, as a result of vanishing cross couplings (corresponding to $G_{1112},G_{2221}=0$ or $\beta=0$), all frequency components at the beat frequency $\omega(\epsilon)$ vanish in the OPM case and the intensity oscillates with the first harmonic $2\omega(\epsilon)$. Note that the modal intensities I_i^0 are given the OPM stationary values found in Sec. III B. Equations (4.12) and (4.13) show that oscillations are in phase. This last point is related to the symmetry in gains and losses for both modes.

The beat frequency $\omega(\epsilon)$ is obtained in Appendix E on the basis of a solvability condition and is given by

$$\omega(\epsilon)=1+\epsilon^2[\gamma G_{12}(I_1^0+I_2^0)-2\beta^2] \tag{4.14}$$

or, in κ units, $\omega=\omega(\epsilon)\Omega$,

$$\omega=\Omega+\frac{A-1}{\Omega}[\gamma_\parallel G_{12}(I_1^{(0)}+I_2^{(0)})-2(A-1)\beta^2]. \tag{4.15}$$

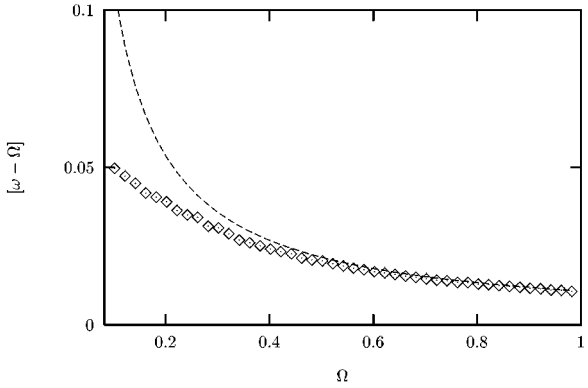

FIG. 6. Values of $\omega-\Omega$ vs Ω for the TEM_{00}-TEM_{70} class B showing frequency pushing effects. $\diamond$ are the numerical results [Eqs. (2.14)] and the dotted line is the theoretical results [Eq. (4.15)]. Same parameters as in Fig. 2 and $\gamma_{\parallel}=0.1$.

We explicitly show that the OPM laser ($\beta=0$) is characterized by frequency pushing phenomena ($\omega>\Omega$). Moreover, this effect is shown to grow with Ω^{-1} (all other parameters constant). The frequency pushing effect has also been observed numerically well above threshold in a TEM_{10}-TEM_{01} laser [25]. On the other hand, the EPM laser may have frequency pulling or pushing effects depending on the parameter values. Varying the relative weight of $\gamma_{\parallel}$ and $A-1$, for instance, the laser exhibits frequency pushing and pulling regimes, though the latter is rather difficult to obtain [for instance, the occurrence of frequency pulling for the TEM_{00}-TEM_{20} case is found for $\gamma_{\parallel}/(A-1)\lesssim 0.05$].

We illustrate our results in the case of the OPM TEM_{00}-TEM_{70} case. The theoretical values of the function $\omega-\Omega$ are plotted in Fig. 6 versus Ω and compared fruitfully with the data obtained by numerical integration of Eqs. (2.14). The characterization of the modal intensities, given in Fig. 7, has been obtained by extracting the maximum and minimum of the periodic signals $I_1(\tau)$ and $I_2(\tau)$ for a given Ω value and by reporting them versus Ω. Our asymptotic theoretical results, obtained in the $\Omega=O(1)$ limit, are shown to be in very good agreement with the numerical data.

According to the results (4.11), the OPM intensity profile

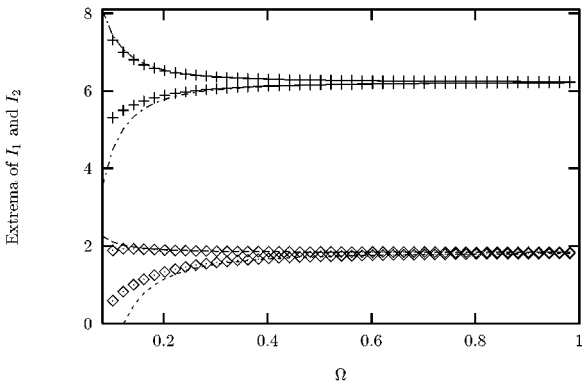

FIG. 7. Maximum and minimum of the periodic modal intensities I_1 and I_2 vs Ω for the TEM_{00}-TEM_{70} class B laser. $\diamond$ and $+$ are numerical results for I_1 and I_2, respectively, and the dotted lines are the theoretical results corresponding to Eq. (4.13).

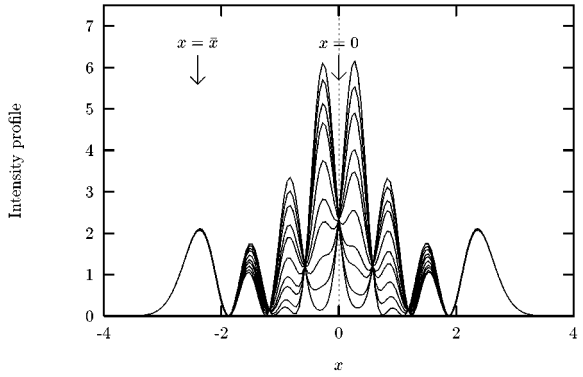

FIG. 8. Intensity profile sampled at different times within period T. At positions $x=0$ and $x=\overline{x}$, the interference term shrinks to zero and the intensities are stationary. Same parameters as in Fig. 2, but $\Omega=1$ and $\gamma_{\parallel}=0.1$.

is characterized by a period T related to twice the beat frequency i.e., $T=\pi/\omega$. Figures 8 and 9 correspond to the intensity profile snapshots taken at different times. Numerical integration at $\Omega=1$ is typical of a ''far from locking regime'' [19] with almost constant modal amplitudes, the only temporal variation being related to mode beating. The intensity profile varies in time according to

$$I(x,y,t)\approx\frac{A-1}{A}[I_1^{(0)}B_1^2(x,y)+I_2^{(0)}B_2^2(x,y)+2\sqrt{I_1^{(0)}I_2^{(0)}}B_1(x,y)B_2(x,y)\cos(\omega t)]. \tag{4.16}$$

It is worth noting here that the temporal variations of $I(x,y,t)$ are related to the last term in Eq. (4.16) and are proportional to $B_1(x,y)B_2(x,y)$. For the TEM_{00}-TEM_{07} case one has $B_1(x,y)B_2(x,y)\to 0$ at $x=0$, where the TEM_{70} mode vanishes and also at $x\approx\overline{x}$ (corresponding to the maximum of the TEM_{70} mode) where the fundamental TEM_{00} mode shrinks to zero. The intensity at these two points is proportional to the modal intensities and is independent (or

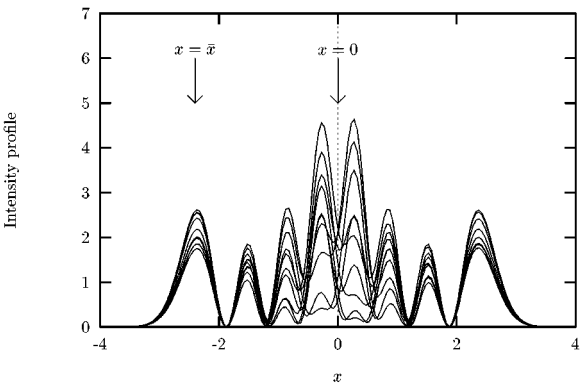

FIG. 9. Intensity profile sampled at different times within period T. The parameters are the same as in Fig. 3. At positions $x=0$ and $x=\overline{x}$, the interference term shrinks to zero, but the corresponding intensities are oscillatory functions proportional to $I_1(\tau)$ and $I_2(\tau)$, respectively.

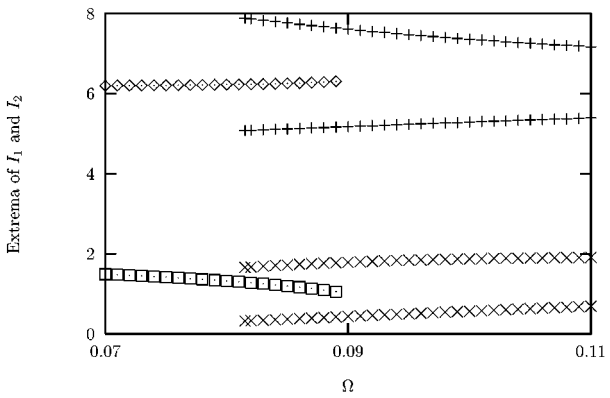

FIG. 10. Extrema of the modal intensities vs Ω for the TEM_{00}-TEM_{70} class *B* laser. □, stationary TEM_{00}; ×, oscillatory TEM_{00}; ◇, stationary TEM_{70}; +, oscillatory TEM_{70} results for I_1 and I_2, respectively. Bistability between periodic and stationary states is found for $\Omega\epsilon[0.08,0.09]$.

almost) of time, as can be seen from Fig. 8. On the other hand, at $\Omega=0.085$, the modal intensities given in Eq. (4.13) have a significant temporal oscillation. The temporal evolution of the intensity profile is related not only to mode beating but also to the oscillating character of the modal intensities [5]. This state, called a prelocking state in the experimental work reported in [19], is shown in Fig. 9.

Figure 10 is a blowup of Figs. 7 and 2 in the interval [0.07,0.11] and clearly evidences bistability between stationary and periodic states (the analysis of bifurcations occurring in Fig. 10 will be considered elsewhere). The periodic solution, which is always stable for high Ω, loses its stability when Ω is lowered (this occurs for $\Omega\approx0.08$) and the system jumps on the bimode stationary branches, which have been analyzed in Sec. III B. Bistability is illustrated by Figs. 3 and 9, which correspond respectively to a stationary and a periodic intensity profile at $\Omega=0.085$ (all parameters are the same in both figures).

B. Class *A* lasers

As usual, the equations for a class *A* laser are obtained in the limit $\gamma_\parallel\gg1$ and the population inversion variables D_{ij} can be adiabatically eliminated. In this limit, the set of equations (2.14) becomes

$$\dot{A}_i=\epsilon\Big(A_i-\sum_j G_{ij}I_jA_i-\sum_j G_{12jj}I_jA_{\bar{i}}\cos\phi - 2G_{iii\,\bar{i}}I_iA_{\bar{i}}\cos\phi-2G_{12}A_iI_{\bar{i}}\cos^2\phi\Big), \quad (4.17)$$

$$\dot{\phi}=1+\epsilon\frac{I_1+I_2}{\sqrt{I_1I_2}}\sin\phi\Big(\sum_j G_{12jj}I_j+2G_{12}A_1A_2\cos\phi\Big),$$

where ϵ is defined in Eq. (4.1). It is worth noting here that in the OPM case these equations simplify into

$$\dot{I}_i=2\epsilon I_i[1-G_{ii}I_i-G_{12}I_{\bar{i}}(\cos(2\phi)+2)], \qquad \dot{\phi}=1+\epsilon G_{12}(I_1+I_2)\sin(2\phi), \quad (4.18)$$

where $I_i=A_i^2$. As was pointed out in Sec. IV A, this expression shows that the OPM laser's dynamics is governed by the variable 2ϕ and modal intensities oscillate at twice the beat frequency.

Repeating the expansion in the same way as in Sec. IV A [see Eqs. (4.4)–(4.6)], one finds from Eqs. (4.17) the solutions

$$A_i(T)=A_i^{(0)}-\epsilon\Big[2G_{iii\,\bar{i}}I_i^{(0)}A_{\bar{i}}^{(0)}\sin T+\beta A_{\bar{i}}\sin T+\frac{G_{12}}{2}A_i^{(0)}I_{\bar{i}}^{(0)}\sin(2T)\Big],$$

$$\phi(T)=T-\epsilon\Big[\beta\frac{I_1^{(0)}+I_2^{(0)}}{\sqrt{I_1^{(0)}I_2^{(0)}}}(1-\cos T)+\frac{G_{12}(I_1^{(0)}+I_2^{(0)})}{2}\times[1-\cos(2T)]\Big], \quad (4.19)$$

where $\beta=\Sigma_jG_{12jj}I_j^{(0)}$ and the $(O\epsilon^0)$ intensities $I_i^{(0)}=[A_i^{(0)}]^2$ are found as

$$I_1^{(0)}=\frac{G_{22}-2G_{12}}{G_{22}G_{11}-4G_{12}^2}, \quad I_2^{(0)}=\frac{G_{11}-2G_{12}}{G_{22}G_{11}-4G_{12}^2}. \quad (4.20)$$

The beat frequency is given by

$$\omega(\epsilon)=1-\epsilon^2\Big[4\beta^2+2\sum_j G_{12jj}^2I_j^{(0)}(I_1^{(0)}+I_2^{(0)})+G_{12}^2(I_1^{(0)2}+I_2^{(0)2}+4I_1^{(0)}I_2^{(0)})\Big], \quad (4.21)$$

or in κ units

$$\omega=\Omega-\frac{(A-1)^2}{\Omega}\Big[4\beta^2+2\sum_j G_{12jj}^2I_j^{(0)}(I_1^{(0)}+I_2^{(0)})+G_{12}^2(I_1^{(0)2}+I_2^{(0)2}+4I_1^{(0)}I_2^{(0)})\Big]. \quad (4.22)$$

These results show that the modal amplitudes have a modulation of order ϵ and the EPM case is characterized by both harmonics ω and 2ω, whereas the former vanishes in the case of the OPM laser. On the other hand, the beat frequency is always pulled ($\omega<\Omega$). From Eq. (4.22) one sees that this pulling effect grows with $(A-1)^2/\Omega^{-1}$. Pulling effects, inherent to class *A* lasers, makes the mode locking in some way more natural in class *A* than in class *B* lasers [10].

Our results are illustrated in the case of the OPM TEM_{00}-TEM_{70} laser. The function $\omega-\Omega$ and the modal intensities are plotted in Figs. 11 and 12, respectively, and show the very good agreement of the theoretical results with the numerical values.

It is interesting to note that, for decreasing Ω, the periodic orbit has larger and larger period [one finds for the OPM case $\omega=0$ when $\Omega/(A-1)=G_{12}(I_1^2+I_2^2+4I_1I_2)^{1/2}$ if Eq. (4.22) is still valid]. It has been checked numerically that the class *A* periodic solutions, stable for high Ω, tends for de-

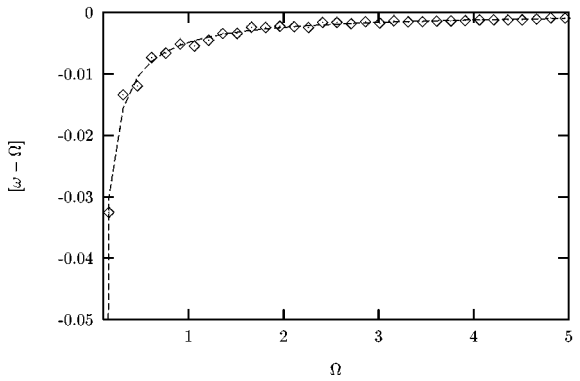

FIG. 11. Plot of $\omega-\Omega$ for the TEM_{00}-TEM_{70} class A laser showing frequency pulling effects. $\diamond$, numerical values; dotted line, theoretical result. The pump parameter is set to $A=1.2$.

creasing Ω to an infinite period orbit homoclinic to the unstable saddle node at detuning value $\Omega_{ho}=\Omega_{max}$ [see, for instance, Eq. (3.4) and Fig. 1]. In contrast to class B lasers, there is no bistability with a locked steady state. A detailed analysis will be given elsewhere.

Let us finally mention here that the present developments are not systematically valid. Assuming $G_{22}<2G_{12}<G_{11}$ in Eqs. (4.20) leads to negative intensities and the developments considered here become irrelevant [26]. If not stationary, numerical simulations show that the behavior of such lasers corresponds to antiphase periodic dynamics [27]. This type of regime is beyond the scope of this paper and will be considered in a future work.

C. Summary

We have analyzed the periodic intensity state in the $\Omega \gg A-1$ limit. The explicit dependence of beat frequency on lasers parameters has been obtained. In particular, we found the analytical expressions for frequency pushing and pulling effects for class B and A lasers, respectively, and showed that these effects grow, for decreasing Ω, as Ω^{-1}.

The modal intensities are sinusoidal functions of time and appear to be very different in the OPM and the EPM case. We first demonstrated that spectral components are different in both cases: The latter (EPM) is related to beat frequency ω, while the former (OPM) is shown to oscillate with pulsation 2ω. On the other hand, the modulation amplitude is shown to be critically different for class A or B, OPM or EPM lasers (orders Ω^2 and Ω, respectively). In this framework we differentiated the ''far from locking regime'' or ''far from degeneracy dynamics,'' where the intensity pattern is governed by beat effects only, and the ''prelocking state'' where the intensity pattern is related to the beat effect and also to the oscillatory behavior of both modal intensities.

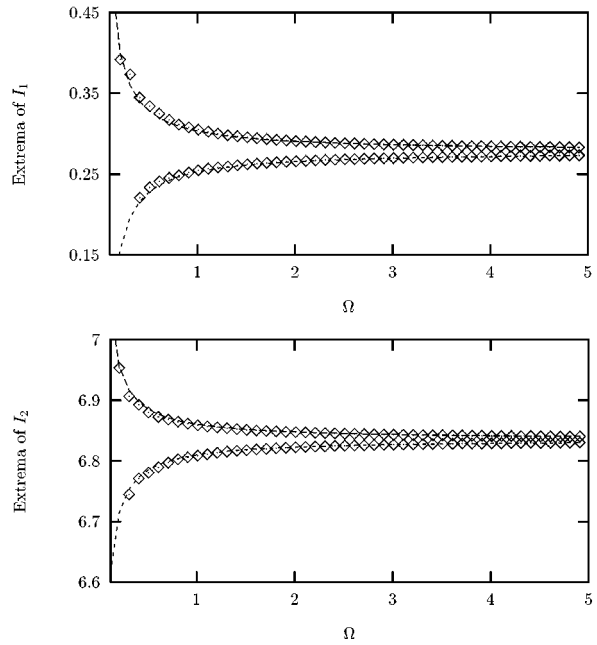

FIG. 12. Maxima of $I_1(t)$ vs Ω for the TEM_{00}-TEM_{70} class A laser. $\diamond$, numerical values; dotted line, theoretical result.

V. CONCLUSION

The laser operating on two transverse modes was analyzed in the framework of a theoretical model valid near threshold and with respect to the detuning between the empty cavity eigenfrequencies Ω (scaled to κ). The dynamics is shown to be extremely sensitive to the laser type, i.e., class A or B laser. We also evidenced the crucial importance played by the relative spatial parity of the modes involved and introduced a clear distinction between what we called the OPM and the EPM laser.

The existence and stability of the locked state have been analyzed. It is shown that the locking threshold is much smaller in the class B than in the class A laser. On the other hand, OPM and EPM lasers are characterized by an optical phase difference $\phi_s=\phi_s(\Omega)$ and by Ω-dependent intensity patterns.

The single-mode state has also been analyzed and is shown to exist for the OPM case only, while its stability is preferably fulfilled for strongly coupled class A lasers. The EPM counterpart of these states has been mentioned and termed a ''quasimonomode.''

Periodic intensity patterns have been studied in the $\Omega=O(1)$ limit [or intermode frequency detuning $O(\kappa)$]. Frequency pushing or pulling effects related to class B and A lasers, respectively, were characterized analytically. The study of the periodic behavior of modal intensities and phase has also been performed and evidences the qualitative distinction between class A or B as well as OPM or EPM lasers.

In the present work, we have used real modal eigenfunctions such as the Hermite-Gauss basis. Indeed, our study could be extended to the ''doughnut'' family of modes. In that case, an analytical description of traveling waves associated with rotating patterns and restless vortices [12,13] could be performed.

Further work could also be devoted to the generalization of the present description in a multimodal approach. In that way, such an extension, if analytically performed, could give a better understanding of the laser dynamics and its dependence with respect to the parameters as well as to the nature of the modes that come into play.

ACKNOWLEDGMENTS

Laboratoire de Spectroscopie Hertzienne is Unité de Recherche Associée au CNRS. Center d'Études et de Recherches Lasers et Applications is supported by the Ministère de la Recherche, Région Nord-Pas de Calais, and Fonds Europien de Développement Économique des Régions.

APPENDIX A: STATIONARY SOLUTION OF THE SYMMETRICAL OPM LASER

1. Class *A* laser

The adiabatic elimination of the inversion variables in Eqs. (2.14) leads, for the OPM laser, to

$$\dot{I}_i = 2I_i[1 - GI_i - I_{\bar{i}}(\cos(2\phi)+2)], \quad \bar{i} = 3 - i,$$

$$\dot{\phi} = \Omega/(A-1) + (I_1 + I_2)\sin(2\phi), \tag{A1}$$

where time is rescaled with respect to the parameter $A-1$ and the modal intensities have been defined by $I_i = G_{12}A_i^2$. We denote by δI_i and $\delta\phi$ the perturbation to the stationary solution and define $X = \delta I_1 + \delta I_2$ and $Y = \delta I_1 - \delta I_2$. We obtain the linearized system

$$\dot{X} = 2[-X + 8I_s^2 \sin(2\phi_s)\,\delta\phi_s],$$

$$\dot{\delta\phi} = X\sin(2\phi_s) + 8I_s\cos(2\phi_s)\,\delta\phi, \tag{A2}$$

and

$$\dot{Y} = 2 - 4GI_sY. \tag{A3}$$

The analysis of eigenvalues show that stability is fulfilled for $I_s \geqslant \langle I \rangle$, i.e., for the upper intensity branch.

2. Class *B* laser

Let us denote by $X = \delta A_1 + \delta A_2$, $Y = \delta A_1 - \delta A_2$, $D = \delta D_{11} + \delta D_{22}$, and $Z = \delta D_{11} - \delta D_{22}, \delta D_{12}, \delta\phi$ the deviation with respect to the stationary solutions $(X_s, Y_s, D_s, Z_s, D_{12s}, \phi_s)$. Time is rescaled with respect to the parameter $A-1$ and $\gamma = \gamma_\parallel/(A-1)$. One obtains from Eqs. (2.14) a set of equations for the variables (Y,Z):

$$\dot{Y} = 2(1 - G_{11}I_s - G_{12}I_s)Y + (G_{12} - G_{11})A_sZ,$$

$$\dot{Z} = -\gamma(Z - 2A_sY) \tag{A4}$$

$(A_s = \sqrt{I_s})$. Stability is fulfilled for $I_s \geqslant 1/2G_{11}, (1-\gamma)/(G_{11}+G_{12})$. The linearized equation for $(X, D, \delta D_{12}, \delta\phi)$ reads

$$\dot{X} = -A_s(G_{12}+G_{11})D - 2G_{12}A_s\cos\phi\,\delta D_{12} + 2I_sA_sG_{12}\sin(2\phi_s)\,\delta\phi,$$

$$\dot{D} = -\gamma(D - 2A_sX),$$

$$\delta\dot{D}_{12} = -\gamma(\delta D_{12} + 2I_s\sin\phi_s - 2A_s\cos\phi_sX),$$

$$\delta\dot{\phi} = 2G_{12}\sin\phi\,\delta D_{12} + 2X\,\delta\phi. \tag{A5}$$

The general discussion of the second set of equations is hard to handle analytically, but, from the characteristic equation, the following results have been obtained.

(i) The Routh Hurwitz criterion leads to a necessary condition for stability: $I_s \geqslant (G+2)/[(G+2)^2 - 1]$. In other words, the lower intensity branch is always unstable.

(ii) At $\Omega = 0$ and for $I_s = I_{max}$, $\phi_s = \pm\pi/2$, Eq. (A5) decouples in a set for (X,D) and for $(\delta D_{12}, \delta\phi)$. The following complex eigenvalues, leading to stability [$\mathrm{Re}(\lambda) < 0$], are obtained:

$$\lambda = -\frac{\gamma_\parallel}{2} \pm 2i\sqrt{\gamma_\parallel(A-1)/(G+1)}, \tag{A6}$$

related to variables $(\delta D_{12}, \delta\phi)$,

$$\lambda = -\frac{\gamma_\parallel}{2} \pm i\sqrt{2\gamma_\parallel(A-1)\frac{G-1}{G+1}}, \tag{A7}$$

related to (Y,Z), and

$$\lambda = -\frac{\gamma_\parallel}{2} \pm i\sqrt{2\gamma_\parallel(A-1)} \tag{A8}$$

for the set (X,D).

(iii) When $\Omega \neq 0$, the analysis can be performed in the limit $\gamma = \gamma_\parallel/(A-1) \to 0$. The characteristic equation is expanded in γ and, from the Routh-Hurwitz criterion, it can be shown that the eigenvalues (A8) lead to a Hopf bifurcation when

$$\Omega = \Omega_{Hopf} = \pm\frac{2(A-1)\sqrt{\gamma(G-1)}}{G+1}. \tag{A9}$$

APPENDIX B: LAMB ANALYSIS OF A BIMODE LASER

Lamb equations for a bimode laser are given by

$$\dot{I}_1 = I_1(a_1 - b_{11}I_1 - b_{12}I_2),$$

$$\dot{I}_2 = I_2(a_2 - b_{22}I_2 - b_{21}I_1), \tag{B1}$$

where I_1 and I_2 are the modal intensities, a_i is the linear gain of mode i, and b_{ij} ($b_{ij} > 0$) are the self- and cross-saturation coefficients. Neglecting phase interactions in Eqs. (2.14) (set $\cos\phi = 0$ and $\sin\phi = 0$) and performing the adiabatic elimination of moments D_{ij}, one gets Eqs. (B1) with $a_1 = a_2 = 1$ and $b_{ij} = G_{ij}$, $b_{12} = b_{21}$. In this framework, it can be shown that the laser has a monomode response, ($I_1 = 0$, $I_2 = 1/G_{22}$) or ($I_2 = 0$, $I_1 = 1/G_{11}$) in the strong-coupling limit, i.e., when $C = G_{12}^2/G_{11}G_{22} > 1$. The bimode solution is given by Eqs. (3.11) and is stable in the weak-coupling limit, i.e., for $C < 1$. It is worth noting here that according to the definition of the overlap integral [see Eq. (2.10)] and from Schwarz inequalities, one has $G_{12}^2 < G_{11}G_{22}$ or $C < 1$ and the bimode study considered here always corresponds, following Lamb criteria, to a weak-coupling situation.

APPENDIX C: OPM STATIONARY STATES

The linear stability analysis of the stationary solutions corresponding to Eqs. (3.10) is performed here. In the case

$\phi_s=0,\pi$, writing $\phi=\phi_s+\tilde{\phi}$ and inserting in Eqs. (2.14), one finds

$$\frac{d\tilde{\phi}}{dt}=2(A-1)G_{12}(I_1+I_2)\tilde{\phi},$$

which shows that these solutions are unstable. In the case $\phi_s=\pm\pi/2$, defining by $\tilde{\phi},\tilde{a}_i,\tilde{d}_{ij}$ the perturbation associated with the stationary values ϕ, A_i, and D_{ij}, respectively, the linearized counterparts of Eqs. (2.14) read

$$\frac{d\tilde{\phi}}{dt}=G_{12}(A-1)\frac{I_1+I_2}{A_1A_2}\sin\phi_s\tilde{d}_{12},$$

$$\frac{d\tilde{d}_{12}}{dt}=\gamma_{\parallel}(-\tilde{d}_{12}+2A_1A_2\sin\phi_s\tilde{\phi}),$$

and

$$\frac{d\tilde{a}_1}{dt}=-(A-1)(G_{11}A_1\tilde{d}_{11}-G_{12}A_1\tilde{d}_{22}),$$

$$\frac{d\tilde{a}_2}{dt}=-(A-1)(G_{22}A_2\tilde{d}_{22}-G_{12}A_2\tilde{d}_{11}),$$

$$\frac{d\tilde{d}_{ii}}{dt}=\gamma_{\parallel}(-\tilde{d}_{ii}+2A_i\tilde{a}_i),\quad i=1,2.$$

The first set of equations gives $\tilde{\phi},\tilde{d}_{12}\sim e^{\lambda t}$, where the eigenvalues λ are given by

$$\lambda=-\frac{\gamma_{\parallel}}{2}\pm\frac{\gamma_{\parallel}}{2}\sqrt{1-8\frac{A-1}{\gamma_{\parallel}}G_{12}(I_1+I_2)}$$

and correspond, as is well known, to aperiodic damped relaxations for class A lasers and to damped oscillations at frequency ω_r,

$$\omega_r=\sqrt{2\gamma_{\parallel}G_{12}(A-1)(I_1+I_2)},\tag{C1}$$

for class B lasers. The second set of equations leads to the eigenvalues

$$\lambda=-\frac{\gamma_{\parallel}}{2}\pm\frac{1}{2}\sqrt{\gamma_{\parallel}^2+4X_{\pm}},$$

$$X_{\pm}=-\gamma_{\parallel}(A-1)[(I_1G_{11}+I_2G_{22})\pm\sqrt{(I_1G_{11}+I_2G_{22})^2-4I_1I_2(G_{11}G_{22}-G_{12}^2)}].$$

It is easily verified that $X_{\pm}$ is real and negative and therefore the real part of λ remains negative provided $A\geqslant 1$.

APPENDIX D: MONOMODE STATIONARY SOLUTIONS

Using Eqs. (2.9) with the variables defined in Eq. (2.11) one has for the OPM case

$$\begin{aligned}\dot{G}_1&=(A-1+i\Omega)G_1-(A-1)[G_{11}D_{11}G_1+G_{12}D_{22}G_1\\&\quad+G_{12}D_{12}G_2],\\ \dot{G}_2&=(A-1)G_2-(A-1)[G_{22}D_{22}G_2+G_{12}D_{11}G_2\\&\quad+G_{12}D_{12}G_1],\end{aligned}\tag{D1}$$

$$\dot{D}_{ii}=-\gamma_{\parallel}(D_{ii}-|G_i|^2),$$

$$\dot{D}_{12}=-\gamma_{\parallel}(D_{12}-G_1G_2^*-G_2G_1^*),$$

where, without loss of generality, we have set $a_2=0$ and $a_1=-\Omega$ [of course performing the transformation $G_i\rightarrow G_i\exp(-ia_2t)$ in Eq. (2.9) leads to Eq. (D1)]. The stationary solutions are given by Eq. (3.19). The linearization of Eq. (D1) leads to a set of equations for the perturbations of the variables G_1,D_{12},

$$\begin{aligned}\dot{\tilde{G}}_1&=(A-1)[1-G_{12}(D_{22})_s]\tilde{G}_1+i\Omega\tilde{G}_1\\&\quad-(A-1)G_{12}(G_2)_s\tilde{D}_{12},\\ \dot{\tilde{D}}_{12}&=\gamma_{\parallel}[\tilde{D}_{12}-(G_2)_s^*\tilde{G}_1-(G_2)_s\tilde{G}_1^*],\end{aligned}\tag{D2}$$

which are decoupled from the remaining variables

$$\begin{aligned}\dot{\tilde{G}}_2&=-(A-1)(G_2)_s[G_{22}\tilde{D}_{22}+G_{12}\tilde{D}_{11}],\\ \dot{\tilde{D}}_{22}&=-\gamma_{\parallel}[\tilde{D}_{22}-(G_2)_s^*\tilde{G}_2-(G_2)_s\tilde{G}_2^*],\end{aligned}\tag{D3}$$

$$\dot{\tilde{D}}_{11}=-\gamma_{\parallel}\tilde{D}_{11}$$

(the label s refers to the stationary values and the tilde refers to the perturbations). The analysis of Eqs. (D2) is easily performed and leads to the stability conditions reported in Eq. (3.21). The second set of equations corresponds to the usual monomode stability analysis. Introducing the intensity $I_2=(G_2)_s^*G_2+(G_2)_sG_2^*$, one finds the monomodelike equations

$$\begin{aligned}\dot{I}_2&=-2(A-1)D_{22},\\ \dot{D}_{22}&=-\gamma_{\parallel}(D_{22}-I_2)\end{aligned}\tag{D4}$$

whose stability is fulfilled above threshold, i.e., when $A\geqslant 1$.

APPENDIX E: ASYMPTOTIC SOLUTIONS FOR CLASS *B* LASERS IN THE $\epsilon \to 0$ LIMIT

To order ϵ, Eqs. (2.14) read

$$\begin{aligned}
\frac{d\phi^{(1)}}{dT} &= -a + \alpha G_{12jk} D_{jk}^{(0)} \sin\phi^{(0)}, \\
\frac{dD_{ii}^{(1)}}{dT} &= -\gamma (D_{ii}^{(0)} - I_i^{(0)}), \\
\frac{dD_{12}^{(1)}}{dT} &= -\gamma (D_{12}^{(0)} - 2A_1^{(0)} A_2^{(0)} \cos\phi^{(0)}), \\
\frac{dA_i^{(1)}}{dT} &= (A_i^{(0)} - G_{iijk} D_{jk}^{(0)} A_i^{(0)} - \cos\phi^{(0)} G_{12jk} D_{jk}^{(0)} A_{\bar{i}}^{(0)})
\end{aligned} \tag{E1}$$

(summation over repeated indices j and k is assumed and $\bar{i} = 3 - i$). The parameter α is defined by

$$\alpha = \frac{I_1^{(0)} + I_2^{(0)}}{\sqrt{I_1^{(0)} I_2^{(0)}}}. \tag{E2}$$

Of course, the solutions of Eqs. (E1) must remain finite in time. One then has to apply solvability conditions, which read, from Eqs. (E1),

$$a = 0, \tag{E3}$$

$$\begin{aligned}
D_{11}^{(0)} = I_1^{(0)} &= \frac{G_{22} - G_{12}}{G_{11} G_{22} - G_{12}^2}, \\
D_{22}^{(0)} = I_2^{(0)} &= \frac{G_{11} - G_{12}}{G_{11} G_{22} - G_{12}^2}, \\
D_{12}^{(0)} &= 0.
\end{aligned} \tag{E4}$$

The solution of Eqs. (E1) reads

$$\begin{aligned}
D_{11}^{(1)}(T) &= D_{11}^{(1)}, \\
D_{12}^{(1)}(T) &= D_{12}^{(1)} + 2\gamma A_1^{(0)} A_2^{(0)} \sin T, \\
\phi^{(1)}(T) &= -\alpha\beta(\cos T - 1), \\
A_1^{(1)}(T) &= A_1^{(1)} - \beta A_2^{(0)} \sin T, \\
A_2^{(1)}(T) &= A_2^{(1)} - \beta A_1^{(0)} \sin T,
\end{aligned} \tag{E5}$$

where we have defined the parameter β as

$$\beta = \sum_j G_{12jj} I_j^{(0)}. \tag{E6}$$

Repeating the development to order ϵ^2, one finds the solvability conditions

$$\begin{aligned}
D_{ij}^{(1)} = A_i^{(1)} &= 0, \quad i,j = 1,2 \\
b &= -2\beta^2 + \gamma (I_1^{(0)} + I_2^{(0)}) G_{12}.
\end{aligned} \tag{E7}$$

Note that the set of equations (E5)–(E7) gives the first corrections to the $O(\epsilon^0)$ EPM solution. In the OPM case, one has $\beta = 0$ and the expansion must be developed further. The $O(\epsilon^2)$ solution reads

$$\begin{aligned}
\phi^{(2)}(T) &= -\frac{\gamma}{2} [I_1^{(0)} + I_2^{(0)}] G_{12} \sin(2T), \\
A_i^{(2)}(T) &= A_i^{(2)} + \frac{\gamma}{2} I_{\bar{i}}^{(0)} A_i^{(0)} G_{12} \cos(2T), \\
D_{ii}^{(2)}(T) &= D_{ii}^{(2)}, \\
D_{12}^{(2)}(T) &= D_{12}^{(2)} + 2\gamma^2 A_1^{(0)} A_2^{(0)} \cos(T).
\end{aligned} \tag{E8}$$

To order ϵ^3, the solvability condition leads to

$$\begin{aligned}
D_{12}^{(2)} &= 0, \\
D_{ii}^{(2)} = 2A_i^{(0)} A_i^{(2)} = I_i^{(2)} &= \frac{\gamma^2 G_{12} (2 G_{12} I_i^{(0)} - 1)}{G_{11} G_{22} - G_{12}^2},
\end{aligned} \tag{E9}$$

$$D_{ii}^{(3)}(T) = D_{ii}^{(3)} + \frac{\gamma^2}{2} I_1^{(0)} I_2^{(0)} G_{12} \sin(2T).$$

[1] L. A. Lugiato, Phys. Rep. **219**, 293 (1992).

[2] C. O. Weiss, Phys. Rep. **219**, 311 (1992).

[3] D. Dangoisse, D. Hennequin, C. Lepers, E. Louvergneaux, and P. Glorieux, Phys. Rev. A **46**, 5955 (1992).

[4] M. Brambilla, F. Battipede, L. A. Lugiato, V. Penna, F. Prati, C. Tamm, and C. O. Weiss, Phys. Rev. A **43**, 5090 (1991); M. Brambilla, L. A. Lugiato, V. Penna, F. Prati, Chr. Tamm, and C. O. Weiss, *ibid.* **43**, 5114 (1991).

[5] J. R. Tredicce, E. J. Quel, A. M. Ghazzawi, C. Green, M. A. Pernigo, L. M. Narducci, and L. A. Lugiato, Phys. Rev. Lett. **62**, 1274 (1989).

[6] L. A. Lugiato, G. L. Oppo, J. R. Tredicce, L. M. Narducci, and

M. A. Pernigo, J. Opt. Soc. Am. B **6**, 1019 (1990).
[7] J. V. Moloney, P. K. Jakobsen, J. Lega, S. G. Wenden, and A. C. Newell, Physica D **68**, 127 (1993).
[8] K. Stalunias, Opt. Commun. **90**, 123 (1992).
[9] K. Stalunias and C. O. Weiss, J. Opt. Soc. Am. B **12**, 1142 (1995).
[10] K. Stalunias, M. F. H. Tarroja, and C. O. Weiss, Opt. Commun. **102**, 69 (1993).
[11] G. Slekys, K. Stalunias, M. F. H. Tarroja, and C. O. Weiss, Appl. Phys. B: Lasers Opt. **59**, 11 (1994).
[12] F. Prati, L. Zucchetti, and G. Molteni, Phys. Rev. A **51**, 4093 (1995).
[13] M. Brambilla, M. Cattaneo, L. A. Lugiato, R. Pirovano, F. Prati, A. J. Kent, G. L. Oppo, A. B. Coates, C. O. Weiss, C. Green, E. J. D'Angelo, and J. R. Tredicce, Phys. Rev. A **49**, 1427 (1994).
[14] C. Tamm, Phys. Rev. A **38**, 5960 (1988).
[15] L. A. Lugiato, C. Oldano, and L. M. Narducci, J. Opt. Soc. Am. B **5**, 879 (1988).
[16] W. E. Lamb, Phys. Rev. **134**, A1429 (1964).
[17] C. L. Tang, H. Statz, and G. de Mars, J. Appl. Phys. **34**, 2289 (1963).
[18] P. Mandel, C. Etrich, and K. Otsuka, IEEE J. Quantum Electron. **29**, 836 (1993).
[19] E. Louvergneaux, G. Slekys, D. Dangoisse, and P. Glorieux (unpublished).
[20] A. E. Siegman, *Lasers* (University Science, Mill Valley, CA, 1986).
[21] The Schwarz inequality implies $G_{11}G_{22} \geqslant G_{12}^2$ and here for the symmetrical case $G_{11} \geqslant G_{12}$.
[22] Unstable solutions are numerically obtained with the AUTO94 computer code from E. J. Doedel, Concordia University, Montreal.
[23] From the definition of the Gauss-Hermite modes, it can be qualitatively understood that $G_{ii} \geqslant G_{jj}$ $(i \leqslant j)$ since higher modes have higher spatial extension and therefore lower average spatial values; the parameter G_{ii} is the spatial integral of the mode to the fourth order and tends to zero for increasing order of the mode. From the same arguments one has $G_{ii}, G_{jj} \geqslant G_{ij}$, $i \neq j$. These qualitative arguments have been checked by explicit numerical integration.
[24] K. Stalunias, G. Slekys, and V. Zehnlé (unpublished).
[25] F. Prati, Ph.D. dissertation, University of Zurich, 1992 (unpublished).
[26] For the TEM_{00}-TEM_{20} case, for instance, one has $G_{11} = 1/\pi$, $G_{22} = 41/64\pi$, and $G_{12} = 3/8\pi$. Equation (4.20) leads to $I_1 < 0$.
[27] T. Erneux and P. Mandel, Phys. Rev. A **52**, 4137 (1995).